The Effects of Gravity and Material Gradation on the Stability of Axially Functionally Graded Cantilevered Pipes Conveying Fluid

Reza Aghazadeh*

ABSTRACT

This study deals with the dynamic problem of axially functionally graded (AFG) fluid conveying cantilevered pipes (FCCPs) aiming at improving stability of such fluid structure interaction systems. The model presented in the current paper also involves the effects of gravity. All material properties of the pipe assumed to be power-law functions of axial coordinate by incorporating a gradient index parameter. By choosing an appropriate value of gradient index different material distribution profiles such as homogeneous, linear, and nonlinear can be achieved. The model, comprised of equation of motion and boundary conditions, is solved by adopting Galerkin method. The influences of gravity, which is related to the mounting orientation of the pipe, longitudinal phase distribution profile, and flow velocity upon dynamics and stability of AFG-FCCPs are discussed in detail through generated numerical results. A special focus is also devoted to determination of critical flow velocity at which the instability occurs.

INTRODUCTION

Along with rapid growth of industrial and technological applications of pipes as fundamental devices for liquid and gas transportations, the mechanical behavior of these elements has been the subject of wide number of researches. Nowadays, the applications of fluid conveying pipes (FCPs) spread from oil exploitation and piping, heat exchanges and hydraulic pipelines to micro- and nano-fluidic devices (ElNajjar and Daneshmand, 2020; Sadeghi-Goughari et al., 2020; Schwengber et al., 2015).

* *Assistant Professor, Department of Aeronautical Engineering, University of Turkish Aeronautical Association, Ankara 06790, Turkey.*

Stability analysis of FCPs play an important role in preventing possible failures such as leakages, fatigue failures and explosions (Sadeghi and Karimi-Dona, 2011). Dynamical problem of FCPs, which has a fluid structure interaction (FSI) nature, aims mainly at finding critical velocities of internal flow at which instability occurs.

It is known that a FCP loses its stability when the flow velocity within it reaches a certain critical value. The instability behaviors of FCPs are significantly influenced by the type of boundary conditions used to support them. A pipe supported at both ends is a conservative system in which static form of instability, called divergence, is expected which leads to buckling of the pipe. A non-conservative cantilever FCP exhibits dynamic type of instability, called flutter, which results in large amplitude transverse vibrations. Although investigation of pipes containing internal flow has a long historical background, most of the recent studies are inspired by Paidoussis (1998). A number of studies deal with linear (Lee and Park, 2006; Xu et al., 2010) and nonlinear (Li et al., 2021; Peng et al., 2018; Tang, Zhen, et al., 2018; Zhang et al., 2016; Zhen et al., 2021) free vibration problems of FCPs. These studies focus on computing natural frequencies of conservative and non-conservative fluid contained pipes with different types of internal flow to investigate the stability of the system. In order to enhance the stability of FCPs, in a study by ElNajjar and Daneshmand (2020) the effects of addition of point masses and springs at different locations along the pipe on the dynamics of vertically and horizontally oriented FCPs are examined. Dagli and Ergut (2019) used Rayleigh theory to investigate mechanics of fluid contained pipes with different non-classical boundary conditions. In studies by Abdollahi et al. (2021) and Jiang et al. (2020) effort is made to address stability and flexural vibration problems of pipes undergoing external and internal fluid loadings simultaneously. Szmidt et al. (2019) used eddy-current damper to stabilize FCPs with fluid flowing with critical velocity within them. On the basis of Green function, closed form solutions are

proposed for forced vibration problem of pipe conveying fluid in a paper by Li and Yang (2014). Tang et al. (2020) studied the thermal effects on wave propagation characteristics of viscoelastic carbon nanotubes conveying fluid with spinning and longitudinal motions. In a study by Tang, Yang, et al. (2018) the fractional dynamics of FCPs made of polymer-like materials which are subjected to the supporting foundation excitation is investigated.

In recent years, along with advances in manufacturing technologies, functionally graded materials (FGMs) have been put forward as an excellent candidate to be used in various engineering applications (Mahamood and Akinlabi, 2017; Petit et al., 2018). Owing to their superior features such as their ability to withstand severe environmental and thermal conditions and low stress concentrations, FGMs have become more preferred choice than traditional homogeneous and laminated composites to be employed in industrial and technological applications in various forms such as beams, plates and shells (Aghazadeh et al., 2018). FGMs can be considered as a modern class of composite materials in which the volume fractions of constituents vary spatially in continuous and smooth manner. Due to these outstanding properties of FGMs, the demand for these materials to be utilized for piping purposes has been raised and consequently much attention has been paid to structural analyses of these elements in the recent decades. A large number of studies regarding dynamics and stability problems of FCPs made of FGMs are devoted to the pipes with through-the-thickness, i.e. radial, variations in material properties (Dehrouyeh-Semnani et al., 2019; Deng et al., 2017; Khodabakhsh et al., 2020; Liu et al., 2019; Reddy et al., 2020; Tang and Yang, 2018b; Zhu et al., 2021; Zhu et al., 2020). Although wide variety of studies pertaining to pure structural problem of axially functionally graded (AFG) beams in absence of fluid flow can be found in the literature (Abo-bakr et al., 2021; Ghayesh, 2018; Li et al., 2017), there is not sufficient effort dealing with AFG pipes conveying fluid. It is worth noting that AFG-FCPs are more suitable for optimization and control purposes in complicated engineering and industrial applications. Moreover, AFG-FCPs require somewhat different modeling and analysis procedures compared to radially functionally graded pipes containing internal flow. To clarify this fact, it can be mentioned that, unlike radially functionally graded pipes, the through-the-length changes of inertia and stiffness coefficients which appear in system of equations of AFG-FCPs must be taken into account when implementing the solution technique. Also, due to lengthwise derivatives of these coefficients, new terms appear in the system of governing equations and boundary conditions. In researches conducted by An and Su (2017) and Zhou et al. (2018) linear dynamics of AFG-FCPs is addressed. Lu et al. (2020)

investigated the effects of dynamic nonlinearities on the fatigue life of FCPs composed of AFG materials. The studies by Ebrahimi-Mamaghani et al. (2020) and Dai et al. (2019) are devoted to stability analysis of AFG-FCPs undergoing thermal loads. Mirtalebi et al. (2019) utilized design flexibility of FGMs for vibration control and manufacturing of AFG fluid contained pipes. Zhao et al. (2021) examined dynamics of AFG-FCPs with conical form. Aghazadeh (2021) developed a new model for dynamic analysis of conservative fluid contained AFG pipes based on a higher order shear deformable pipe theory which properly estimates transverse shear stress distribution. A novel type of FGM structures with improved functionality and design flexibility are recently put forward which possess continuous change in material properties along two different directions (Aghazadeh, 2020; Tang et al., 2019; Tang, Ma, et al., 2021; Tang, Wang, et al., 2021). A study by Tang and Yang (2018a) focused on the examination of dynamics and stability behaviors of FCPs made of bi-directional FGMs.

One of the significant aspects that should be considered in modeling and analysis of FCPs, especially when it is oriented vertically, is forces due to gravity. The effect of gravity is more pronounced for long pipes made of materials with low stiffness. There are numerous studies in the literature addressing influences of gravitational forces on the stability of FCPs (Chen et al., 2020; Ebrahimi-Mamaghani et al., 2019; ElNajjar and Daneshmand, 2020; Ge et al., 2019; Rivero-Rodriguez and Pérez-Saborid, 2015) all of which, to the best of author's knowledge, are conducted for homogeneous pipes. In the current study, the terms which appear in the equation of motion of FCPs are retreated and modified to be applicable for AFG pipes.

The motivation of the present study is to put forward a dynamical model for predicting stability characteristics of AFG-FCPs by taking the gravity effects into account. A power-law function, employing a gradient index, is used to capture the lengthwise variations of material properties. The system including equation of motion and boundary conditions is derived and then solved by adopting Galerkin method. The parametric analyses are carried out for a cantilevered metal-ceramic pipe which displays flutter type of instability. Detailed numerical analyses are conducted to delineate the influences of phase distribution profile, gravitational force, and flow velocity upon stability and vibrational features of axially functionally graded fluid conveying cantilevered pipes (AFG-FCCPs). Moreover, a special focus is made on estimating critical values of the flow velocities at which the system loses its stability.

FORMULATION

Figure 1 illustrates an AFG-FCCP with length L, inner and outer radii r_i and r_o, in three different oriented configurations, i.e., horizontal, vertically upward and vertically downward. A fluid with velocity Γ flows within the pipe. A gradient color scale is used to indicate the smooth material gradation through the AFG pipe length. In absence of pressurization, gravity, internal damping and external tension, the model for homogeneous fluid contained pipe which is proposed by Paidoussis (1998) can be rewritten for AFG pipes by considering the material properties as functions of x_1-direction, as follows

$$I\frac{\partial^2}{\partial x_1^2}\left(E(x_1)\frac{\partial^2 w}{\partial x_1^2}\right)+m_f\Gamma^2\frac{\partial^2 w}{\partial x_1^2}$$
$$+\rho(x_1)A\frac{\partial^2 w}{\partial t^2}+m_f\frac{\partial^2 w}{\partial t^2}+2m_f\Gamma\frac{\partial^2 w}{\partial x_1\partial t}=0 \tag{1}$$

where t is the time, and w denotes transverse displacement of the pipe. The modulus of elasticity and density of pipe material are denoted by E and ρ, respectively. $m_f=\rho_f A_f$ designates the fluid mass per unit length with A_f and ρ_f representing the flow cross section and fluid density, respectively. A is the cross-sectional area and I stands for moment of inertia of the pipe. In addition to equation of motion given by Eq. (1), the following boundary conditions must be satisfied for a cantilevered pipe

At $x_1=0$ $\quad w=\dfrac{\partial w}{\partial x_1}=0,$ (2.a)

At $x_1=L$ $\quad \dfrac{\partial^3 w}{\partial x_1^3}=\dfrac{\partial^2 w}{\partial x_1^2}=0.$ (2.b)

The governing equation expressed by Eq. (1) can be derived by Newtonian or Hamiltonian approaches. In the present study, the term associated with gravity will be derived using Hamilton's principle which, in absence of work done by external forces, postulates that

$$\delta\int_{t_1}^{t_2}(K-U)\,dt=0. \tag{3}$$
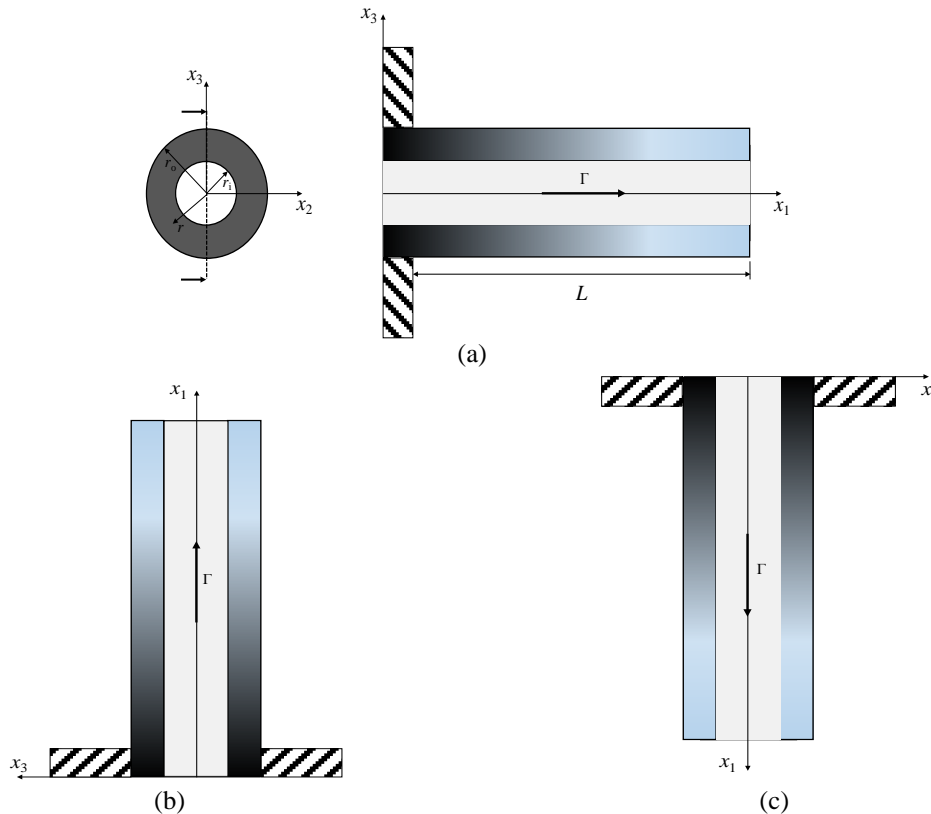
Figure 1. Schematic of axially functionally graded fluid conveying cantilevered pipe oriented (a) horizontally, (b) vertically upward and (c) vertically downward.

where K and U are kinetic and potential energies, respectively. K is comprised of kinetic energies

associated with motions of both pipe and fluid. U involves strain energy of the pipe and potential energy due to gravity. Note that, the terms regarding kinetic strain energies have already appeared in Eq (1). For an AFG-pipe with nonuniform lengthwise material distribution, the gravitational potential energy U_g can be written as

$$
\begin{aligned}
U_g &= \frac{1}{2}\int_0^L \int_0^{x_1} \left(m_f + \rho(x_1)A\right)g\left(\frac{\partial w}{\partial x_1}\right)^2 dx_1 dx_1 \\
&= \left[\frac{1}{2}x_1 \int_0^{x_1}\left(m_f + \rho(\eta)A\right)g\left(\frac{\partial w}{\partial x_1}\right)^2 dx_1\right]_0^L \\
&\quad - \frac{1}{2}\int_0^L \left(m_f + \rho(x_1)A\right)g x_1\left(\frac{\partial w}{\partial x_1}\right)^2 dx_1 \\
&= \frac{1}{2}g\int_0^L \left(m_f + \rho(x_1)A\right)(L - x_1)\left(\frac{\partial w}{\partial x_1}\right)^2 dx_1
\end{aligned}
\tag{4}
$$

Taking the variation of U_g, applying integration by parts, and introducing the resulted term into Eq. (3), one can obtain the term pertaining to gravity effects. Consequently, governing equation given by Eq. (1) can be rewritten to comprise gravitational forces as follows

$$
\begin{aligned}
&I\frac{\partial^2}{\partial x_1^2}\left(E(x_1)\frac{\partial^2 w}{\partial x_1^2}\right) + m_f\Gamma^2\frac{\partial^2 w}{\partial x_1^2} \\
&- g\frac{\partial}{\partial x_1}\left\{\left\{\left(m_f + \rho(x_1)A\right)(L - x_1)\right\}\frac{\partial w}{\partial x_1}\right\} \\
&+ \rho(x_1)A\frac{\partial^2 w}{\partial t^2} + m_f\frac{\partial^2 w}{\partial t^2} + 2m_f\Gamma\frac{\partial^2 w}{\partial x_1 \partial t} = 0.
\end{aligned}
\tag{5}
$$

Eq. (5) is converted to the one derived by Paidoussis (1998) once the variation of material constants in axial direction is disregarded. Introducing the following dimensionless parameters

$$
\xi = \frac{x_1}{L}, \quad \eta = \frac{w}{L}, \quad \tau = \left[\frac{E_0 I}{m_f + \rho_0 A}\right]^{1/2}\frac{t}{L^2},
$$

$$
\bar{E}(\xi) = \frac{E(\xi)}{E_0}, \quad \bar{\rho}(\xi) = \frac{\rho(\xi)}{\rho_0}, \quad u = \left(\frac{m_f}{E_0 I}\right)^{1/2}L\Gamma,
$$

$$
\beta_p = \frac{\rho_0 A}{m_f + \rho_0 A}, \quad \beta_f = \frac{m_f}{m_f + \rho_0 A},
$$

$$
\kappa_p = \frac{\rho_0 A L^3}{E_0 I}g, \quad \kappa_f = \frac{m_f L^3}{E_0 I}g,
\tag{6}
$$

yields dimensionless form of Eq. (5):

$$
\begin{aligned}
&\frac{\partial^2}{\partial \xi^2}\left(\bar{E}(\xi)\frac{\partial^2 \eta}{\partial \xi^2}\right) + u^2\frac{\partial^2 \eta}{\partial \xi^2} \\
&- \left(\kappa_f + \kappa_p\bar{\rho}(\xi)\right)(1-\xi)\frac{\partial^2 \eta}{\partial \xi^2} \\
&+ \left(\kappa_f + \kappa_p\bar{\rho}(\xi)\right)\frac{\partial \eta}{\partial \xi} - \kappa_p\frac{\partial\bar{\rho}(\xi)}{\partial \xi}(1-\xi)\frac{\partial \eta}{\partial \xi} \\
&+ \beta_p\bar{\rho}(\xi)\frac{\partial^2 \eta}{\partial \tau^2} + \beta_f\frac{\partial^2 \eta}{\partial \tau^2} + 2u\sqrt{\beta_f}\frac{\partial^2 \eta}{\partial \xi \partial \tau} = 0.
\end{aligned}
\tag{7}
$$

where the constituent at the left side of the pipe, $x_1 = 0$, is indicated by subscript '0'.

NUMERICAL SOLUTION

In the present study, Galerkin method, which is one of the powerful techniques in analyzing continuous systems, is adopted to solve governing equation expressed by Eq. (7). Using this method, the dependent variable $\eta(\xi,\tau)$ is approximated as sum of separated functions of space and time variables:

$$
\eta(\xi,\tau) = \sum_{r=1}^{\infty} \varphi_r(\xi)q_r(\tau)
\tag{8}
$$

$q_r(\tau)$ here designate generalized coordinates of the discretized system and $\varphi_r(\xi)$ are dimensionless eigenfunctions of the pipe under consideration which must satisfy the corresponding boundary conditions. Substituting Eq. (8) into Eq. (7), followed by multiplying the results by $\varphi_s(\xi)$ and then integrating over the domain [0,1] yields

$$
\begin{aligned}
\sum_{r=1}^{\infty}\Big\{ &\lambda_r^4\delta_{sr}^E q_r + 2e_{sr}^{E'}q_r + c_{sr}^{E''}q_r + u^2 c_{sr}q_r \\
&- \kappa_f\left(c_{sr} - d_{sr}\right)q_r + \kappa_f b_{sr}q_r - \kappa_p\left(c_{sr}^\rho - d_{sr}^\rho\right)q_r \\
&+ \kappa_p b_{sr}^\rho q_r - \kappa_p\left(b_{sr}^{\rho'} - f_{sr}^{\rho'}\right)q_r \\
&+ \beta_p\delta_{sr}^\rho\ddot{q}_r + \beta_f\delta_{sr}\ddot{q}_r + 2u\sqrt{\beta_f}b_{sr}\dot{q}_r\Big\} = 0,
\end{aligned}
\tag{9}
$$

where λ_r are the rth dimensionless eigenvalues of the pipe and a dot denotes differentiation with respect to dimensionless time τ. The set of constants appearing in Eq. (9) are defined as follows

$$\delta_{sr} = \int_0^1 \varphi_s \varphi_r \, d\xi, \quad b_{sr} = \int_0^1 \varphi_s \varphi_r' \, d\xi,$$

$$c_{sr} = \int_0^1 \varphi_s \varphi_r'' \, d\xi, \quad d_{sr} = \int_0^1 \varphi_s \varphi_r'' \xi \, d\xi,$$

$$\delta_{sr}^Z = \int_0^1 \overline{Z}(\xi) \varphi_s \varphi_r \, d\xi, \quad b_{sr}^Z = \int_0^1 \overline{Z}(\xi) \varphi_s \varphi_r' \, d\xi,$$

$$b_{sr}^{Z'} = \int_0^1 \frac{\partial \overline{Z}(\xi)}{\partial \xi} \varphi_s \varphi_r' \, d\xi, \quad c_{sr}^Z = \int_0^1 \overline{Z}(\xi) \varphi_s \varphi_r'' \, d\xi,$$

$$c_{sr}^{Z''} = \int_0^1 \frac{\partial^2 \overline{Z}(\xi)}{\partial \xi^2} \varphi_s \varphi_r'' \, d\xi, \quad d_{sr}^Z = \int_0^1 \overline{Z}(\xi) \varphi_s \varphi_r'' \xi \, d\xi,$$

$$e_{sr}^{Z'} = \int_0^1 \frac{\partial \overline{Z}(\xi)}{\partial \xi} \varphi_s \varphi_r'' \, d\xi, \quad f_{sr}^{Z'} = \int_0^1 \frac{\partial \overline{Z}(\xi)}{\partial \xi} \varphi_s \varphi_r' \xi \, d\xi$$

$$(10)$$

where Z represents a typical material property such as E and ρ, and a prime stands for differentiation with respect to dimensionless spatial coordinate ξ. From the first relation of Eq. (10) for δ_{sr} being Kronecker's delta, it can obviously be seen that eigenfunctions satisfy orthogonality conditions. It is worth noting that, except b_{sr}, c_{sr}, and d_{sr} whose evaluation procedures are provided by Paidoussis (1998), the other constants are new and exist due to dependency of material properties to axial coordinate, and can be evaluated in a similar manner.

By defining vector **q** containing the unknown generalized coordinates, Eq. (9) is recast into the following standard form

$$\mathbf{M\ddot{q}} + \mathbf{C\dot{q}} + \mathbf{Kq} = \mathbf{0} \tag{11}$$

K, **C**, and **M** here are stiffness, damping, and mass matrices, respectively, and are given by the following expressions

$$\mathbf{M} = \beta_p \mathbf{I}_\rho + \beta_f \mathbf{I}, \tag{12.a}$$

$$\mathbf{C} = 2u\sqrt{\beta_f} \mathbf{B}, \tag{12.b}$$

$$\mathbf{K} = \Lambda_E + 2\mathbf{E}_{E'} + \mathbf{C}_{E''} + u^2 \mathbf{C} - \kappa_f (\mathbf{C} - \mathbf{D})$$
$$+ \kappa_f \mathbf{B} - \kappa_p (\mathbf{C}_\rho - \mathbf{D}_\rho) + \kappa_p \mathbf{B}_\rho - \kappa_p (\mathbf{B}_{\rho'} - \mathbf{F}_{\rho'}), \tag{12.c}$$

where **I** is the identity matrix, Λ_E contains the components of δ_{sr}^E with its elements on rth column multiplied by λ_r^4 and $\mathbf{I}_\rho$, **B**, $\mathbf{B}_\rho$, $\mathbf{B}_{\rho'}$, **C**, $\mathbf{C}_\rho$, $\mathbf{C}_{E''}$, **D**, $\mathbf{D}_\rho$, $\mathbf{E}_{E'}$ and $\mathbf{F}_{\rho'}$ are matrices with elements δ_{sr}^ρ, b_{sr}, b_{sr}^ρ, $b_{sr}^{\rho'}$, c_{sr}, c_{sr}^ρ, $c_{sr}^{E''}$, d_{sr}, d_{sr}^ρ, $e_{sr}^{E'}$ and $f_{sr}^{\rho'}$, respectively.

For a self-excited motion the unknown generalized coordinates **q** can be defined as

$$\{q\} = \{q^*\} e^{i\omega\tau} = \{q^*\} e^{\Omega\tau}, \tag{13}$$

where ω and Ω are dimensionless eigenfrequencies and eigenvalues, respectively, and $\{q^*\}$ denotes corresponding vibration amplitudes or eigenvectors. Substitution of Eq. (13) into Eq.(11), leads to the following standard generalized eigenvalue problem

$$\{\mathbf{K} + \Omega\mathbf{C} + \Omega^2\mathbf{M}\} \{q^*\} = \mathbf{0}. \tag{14}$$

Letting determinant of the coefficient matrix of eigenvalue problem equal to zero, one can achieve the nontrivial solution of Eq. (14)

$$\det\{\mathbf{K} + \Omega\mathbf{C} + \Omega^2\mathbf{M}\} = \mathbf{0}. \tag{15}$$

The eigenfrequencies obtained by implementing the abovementioned procedures, are complex values due to the damping introduced by fluid flow. Imaginary and real parts of ω, denoted by $\text{Im}(\omega)$ and $\text{Re}(\omega)$, represent decaying rate and oscillation frequency of the system, respectively. When flow velocity reaches a certain critical value at which $\text{Im}(\omega) < 0$, the FCP exhibits unstable behavior.

For a cantilevered pipe, which is studied in the current research, eigenfunctions are given as

$$\varphi_r(\xi) = \cosh \lambda_r \xi - \cos \lambda_r \xi - \sigma_r (\sinh \lambda_r \xi$$
$$- \sin \lambda_r \xi), \quad \text{where} \quad \sigma_r = \frac{\sinh \lambda_r - \sin \lambda_r}{\cosh \lambda_r + \cos \lambda_r} \tag{16}$$

λ_r are dimensionless eigenvalues of a cantilever beam and are computed as the solution of the following characteristic equation

$$\cos \lambda_r \cosh \lambda_r + 1 = 0 \tag{17}$$

NUMERICAL RESULTS

In this section, based on Galerkin solution technique, numerical results pertaining to dynamic problem of a metal-ceramic AFG-FCCP are reported. Axial variations of AFG pipe constituents are captured by assuming it to be made of stainless steel (SUS304) at upstream, $x_1 = 0$, and silicon nitride (Si$_3$N$_4$) at downstream, $x_1 = L$; with following material properties: $E_0 = 201$ GPa, $E_L = 348$ GPa, $\rho_0 = 8166$ kg/m^3, $\rho_L = 2370$ kg/m^3, where subscripts '0' and 'L' are used to indicate properties at $x_1 = 0$ and $x_1 = L$, respectively. The effective typical material property denoted by Z, including E and ρ smoothly varies according to a power-law function of axial coordinate

$$Z(x_1) = Z_0 \left(1 + \left(\frac{Z_L}{Z_0} - 1\right)\left(\frac{x_1}{L}\right)^\alpha\right) \tag{18}$$

where α is a non-negative parameter called power-law index which prescribes through-the-length material distribution pattern. A fully ceramic pipe can be modeled by letting $\alpha = 0$ whereas $\alpha = 1$ implies a linear lengthwise change of properties, from metal to ceramic. Choosing a value other than 0 and 1 as power-law index yields a nonlinear gradation pattern. The variations of E and ρ along the pipe length for different values of α are illustrated in Figure 2.

(a)

(b)
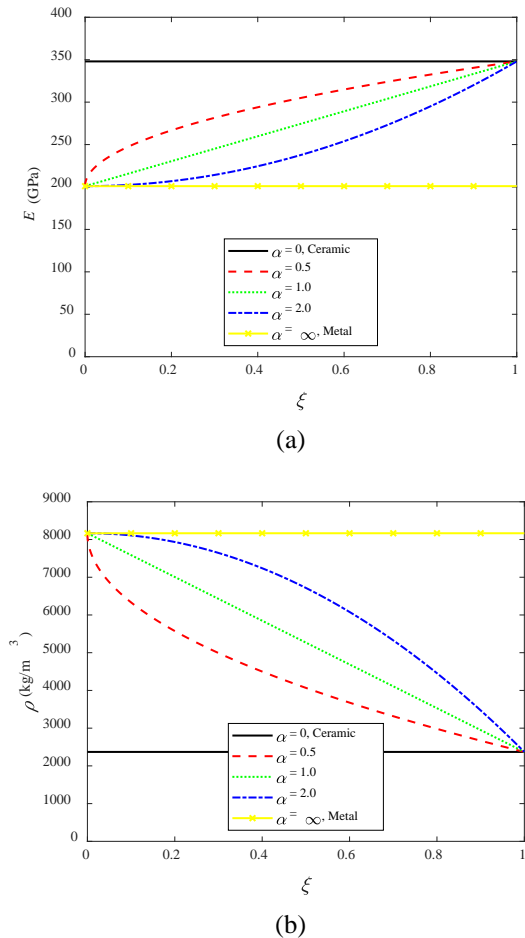
Figure 2. Longitudinal variations of material properties (a) modulus of elasticity E and (b) density ρ along AFG-FCP

The convergence and verification analyses of the numerical results generated based on the procedures developed in the current study is conducted by providing critical flow velocities for homogeneous and axially functionally graded FCCPs in Table 1. Excellent agreement can be seen between the results computed by utilizing the techniques presented in this study with those provided by Paidoussis (1998). The results produced by employing different numbers of Galerkin terms N suggest that the convergences can be achieved with N

$= 3$ for homogeneous and $N = 5$ for AFG pipes.

Figure 3 illustrates the influences of dimensionless mass ratio β_f upon dimensionless critical flow velocity u_{cr} in different values of gradient index α. Note that the u_{cr}-values for the current non-conservative cantilevered system corresponds to flutter type of instability which occurs when $\mathrm{Im}(\omega) < 0$ and $\mathrm{Re}(\omega) > 0$. Further, it should be mentioned that various industrial piping systems are recognized by their β_f-values; e. g. for a carbon steel pipe used in crude oil and natural gas pipelines, β_f is approximately equal to 0.165 and 0.0001, respectively (ElNajjar and Daneshmand, 2020). κ_p and κ_f are dimensionless terms associated with gravity effects due to pipe and fluid weights, respectively. In the current study, for the sake of avoiding complexity, κ_p and κ_f are assumed to be equal, $\kappa_p = \kappa_f = \kappa$. In a pipe mounted horizontally, as depicted in Figure 1.a, the gravity effect is neglected and hence κ is taken as zero. When the pipe is oriented vertically upward as depicted in Figure 1.b, the flow velocity and gravity are in opposite directions and the gravitational forces induce compression on pipe, and consequently $\kappa < 0$ for this system. $\kappa > 0$ represents a pipe with a vertically downward orientation, see Figure 1.c, meaning that the flow velocity is in the same direction as gravity, and the pipe is acted by gravity-induced tension. Inspecting Figure 3 it can be found that u_{cr} is an increasing function of β_f. Moreover, increase in the value of κ leads to corresponding increase in u_{cr}, postulating that the system is more stabilized in higher values of κ. This fact can be justified by knowing that as κ gets larger the restoring force becomes higher and hence stabilizes the system. In an upstanding pipe where $\kappa < 0$ the restoring force diminishes, and the system loses stability. Comparing the results obtained for different values of dimensionless gravity parameter κ, it can be understood that, in a certain value of power-law index, the trend is preserved and the increase in u_{cr} as a result of increase in β_f takes place in a similar manner.

Table 1. Critical flow velocities of horizontal AFG-FCCPs with $\beta_f = 0.2$, and $\kappa_p = \kappa_f = 0$.

Gradient index α	Present, $N = 2$	Present, $N = 3$	Present, $N = 4$	Present, $N = 5$	Present, $N = 6$	Paidoussis (1998)
$\alpha = \infty$ (fully metal)	5.42	5.60	5.60	5.60	5.60	5.60
$\alpha = 2.0$	8.80	7.05	6.87	6.86	6.86	-

(a)

(b)

(c)

(d)

(e)
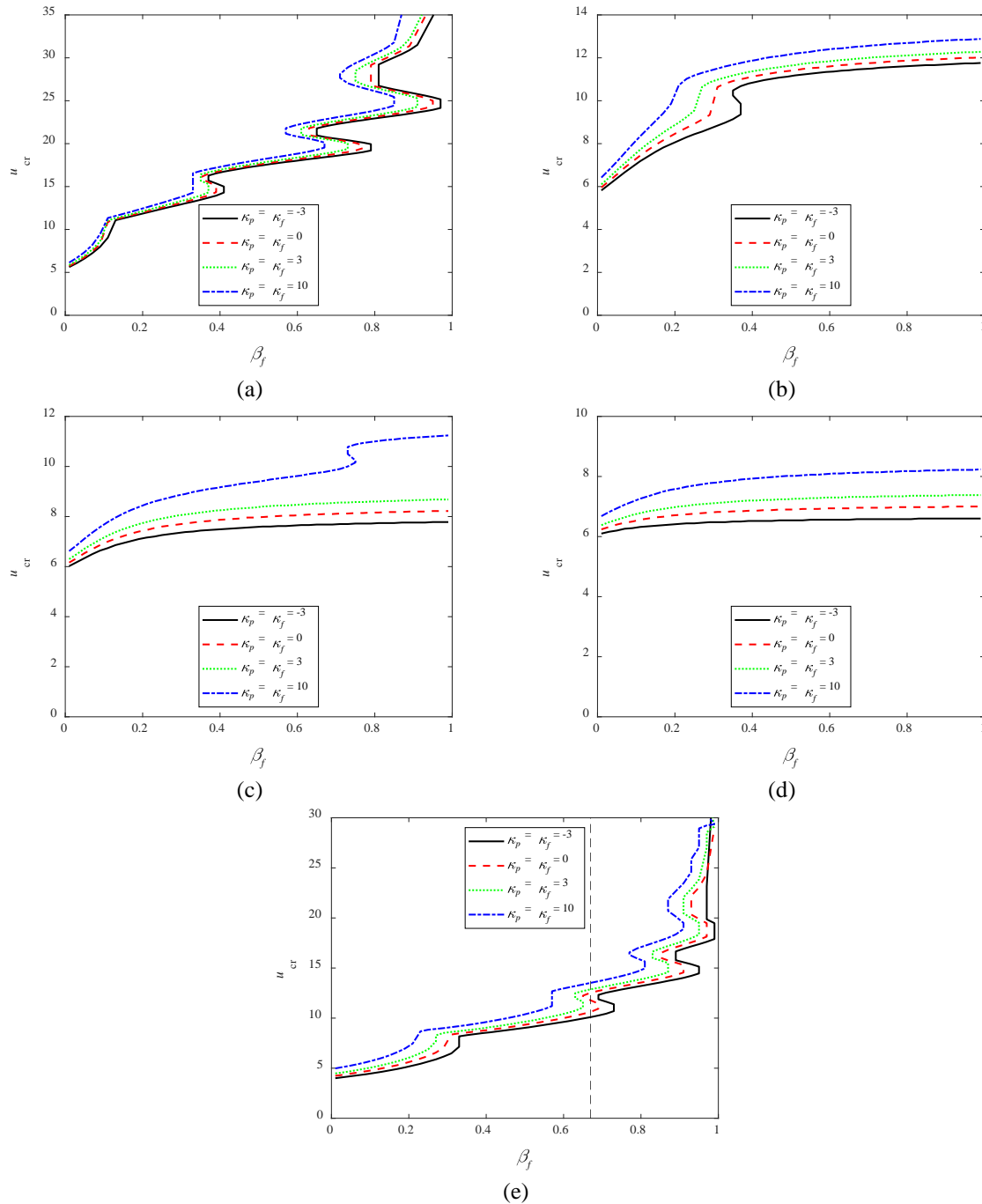
Figure 3. Critical flow velocities of AFG-FCCPs with (a) $\alpha = 0$ (fully ceramic), (b) $\alpha = 0.5$, (c) $\alpha = 1$, (d) $\alpha = 2$, (e) $\alpha = \infty$ (fully metal).

In order to investigate the dynamic and stability behaviors of an AFG-FCCP in different values of gradient index α, the curves of Figure 3 belonging to horizontal pipe are replotted in Figure 4. Generally, smaller values of α indicate a ceramic-dominant pipe and hence yield enhanced stability. However, an exception can be seen at a certain value of β_f, in this case at $\beta_f \approx 0.3$, where the pure metal pipe starts to display more stabilized behavior compared to other pipes with $\alpha \neq 0$. In addition to above-mentioned

findings, it can be observed that in some cases S-shaped segments exist in u_{cr}-β_f curves at which at certain values of β_f three corresponding values of u_{cr} are seen. One of the examples of this phenomena is shown by a vertical dashed line drawn at $\beta_f = 0.67$ in Figure 3.e which intersects the curve for horizontal pipe, $\kappa_p = \kappa_f = 0$, at three points. The S-shaped regions imply destabilization – restabilization – destabilization (D-R-D) behavior meaning that the system gains stability at $u > u_{cr}$ and then, by further

increasing the flow velocity, it loses its stability again.
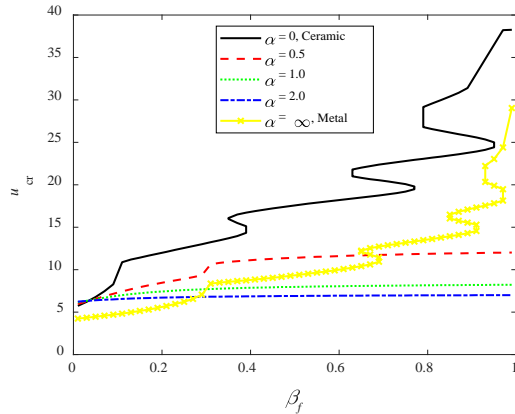
Figure 4. Critical flow velocity of AFG-FCCP with $\kappa_p = \kappa_f = 0$.

Depicted in Figure 5 are the Argand diagrams for horizontally mounted AFG cantilevered pipes with different α-values which are generated by taking $\beta_f = 0.67$. For the sake of clarity, the flow velocity values are specified close to the corresponding data points, and some regions are magnified. Argand diagrams are useful for analyzing the effects of velocity on vibrational features of systems such as eigenfrequencies and instability. The critical flow velocity can be found from Argand diagrams by determining the velocities at which the curves intersect $\mathrm{Re}(\omega)$-axis and hence $\mathrm{Im}(\omega)$ gets negative. From Figure 5 it can be understood that in all values of power-law index, the smallest u_{cr} is seen to belong to the first mode, and at a higher value of flow velocity than critical one, an AFG-FCCP experiences instability in its second mode of vibration. Further, it can be clearly observed that all curves start from $\mathrm{Im}(\omega)=0$, i. e. $\mathrm{Re}(\omega)$-axis, when $u = 0$, which can be justified by the fact that damping of the system originates from the term $2u\sqrt{\beta_f}\,\partial^2\eta / \partial\xi\partial\tau$ in Eq. (7) and in absence a flow it becomes zero, representing an undamped system. For nonzero values of u the damping exists and consequently $\mathrm{Im}(\omega)$ becomes nonzero. Moreover, the D-R-D region discussed in the foregoing paragraph can also be seen in Figure 5.e, where the Argand curve for the first mode intersects the horizontal axis three times. For the purpose of investigating gravity effects, the results of Figure 5.d for $\alpha = 2$ is regenerated in Figure 6 for upstanding AFG-FCCP with $\kappa = -3$. The critical flow velocities for these two cases can be read from Argand diagrams which also are the same as those of Figure 3.d. Comparing the Argand diagrams of horizontally and vertically oriented AFG-FCCPs, one can figure out that the trend is preserved in both cases.

(a)

(b)
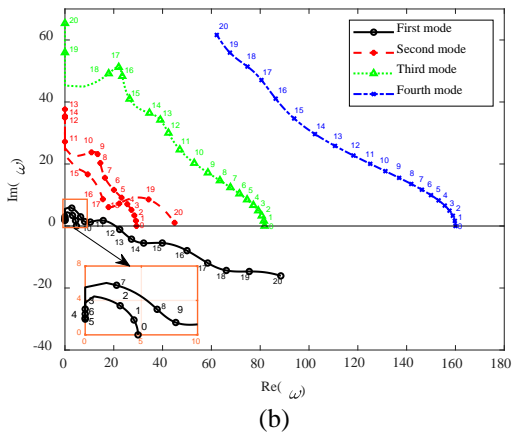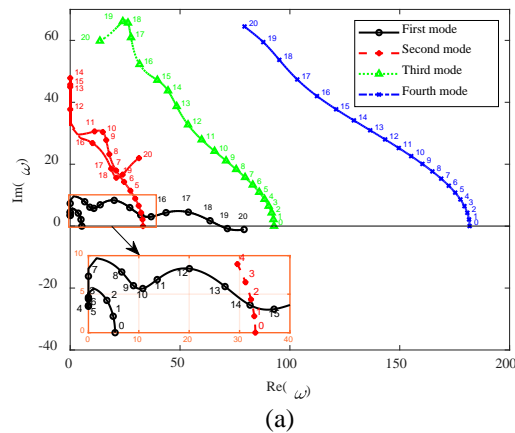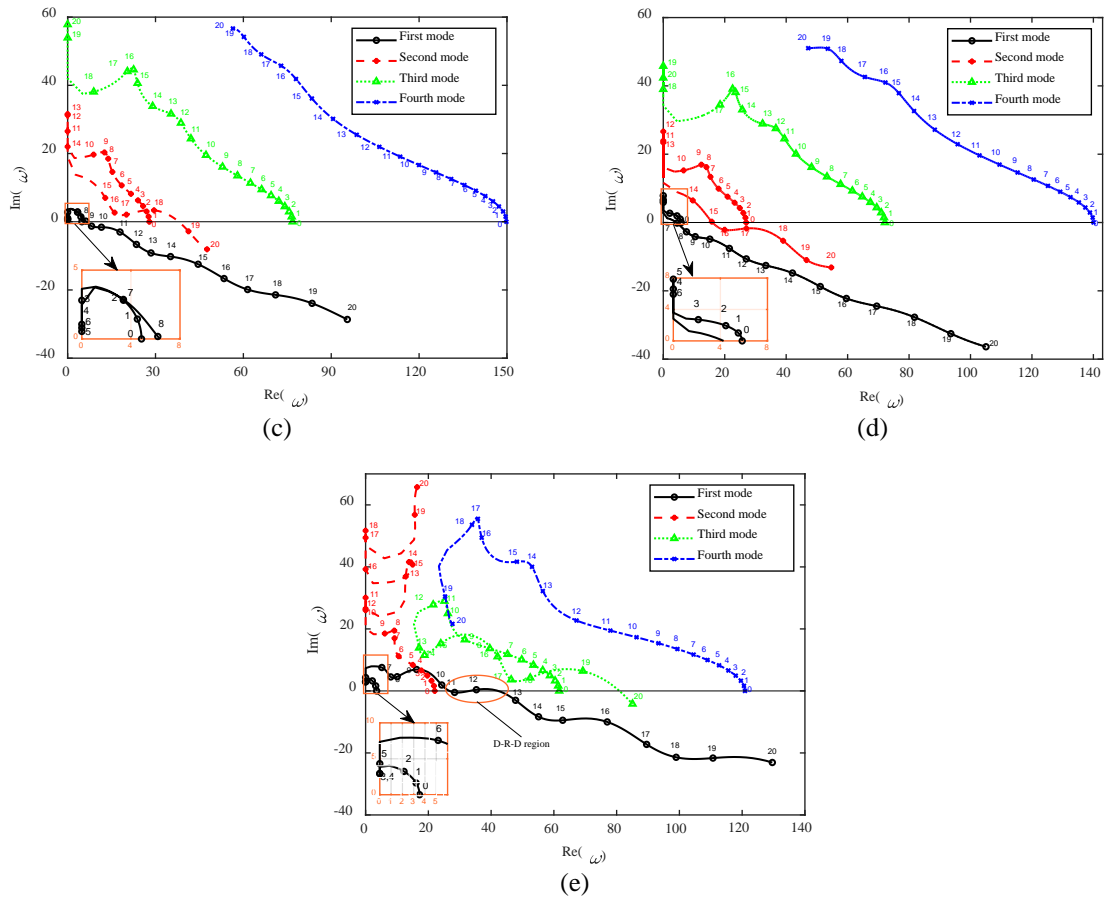
Figure 5. Argand diagrams for AFG-FCCPs with $\beta_f = 0.67$, $\kappa_p = \kappa_f = 0$, and (a) $\alpha = 0$ (fully ceramic), (b) $\alpha = 0.5$, (c) $\alpha = 1$, (d) $\alpha = 2$, (e) $\alpha = \infty$ (fully metal).
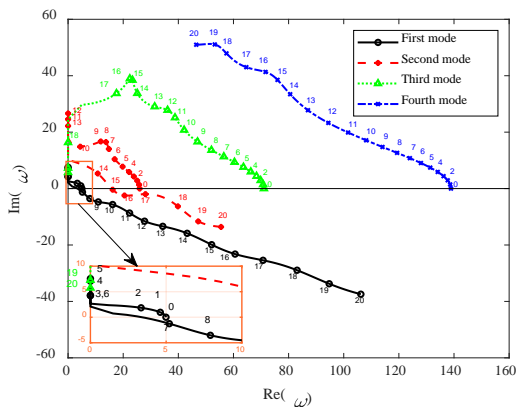
Figure 6. Argand diagram for an AFG-FCCP with $\beta_f = 0.67$, $\kappa_p = \kappa_f = -3$, and $\alpha = 2$.

CONCLUSION

The current study aims at putting forward a new model and analysis procedure for dynamic and stability problems of AFG-FCCPs in presence of gravity effects. After derivation of the system of governing equation and boundary conditions, it is solved by employing Galerkin method which necessitates the evaluation of new integrals due to axial variation of material constants. Through-the-length phase distribution pattern is assigned using a power-law-function incorporating a power-law index which delineates the form of material variation. u_{cr}-β_f plots as well as Argand diagrams in different values of dimensionless gravity term κ and gradient index α are provided to investigate the effects of material gradation and gravity on the dynamics of AFG-FCCPs including critical flow velocities and frequencies of such FSI systems.

The numerical results reveal that power-law index α has a significant effect on stability behavior of the AFG pipes which make functionally graded materials to be considered as a promising choice for fluid conveying applications, especially for control and optimization purposes. The variations of u_{cr} with respect to α depends on the constituents used to fabricate the AFG pipe at its left and right ends. For the current metal-ceramic AFG pipe better stability performance is observed in smaller α-values with ceramic phase being dominant. The exception for this trend is seen to occur at some values of dimensionless mass β_f at which a homogeneous metal

pipe exhibits more stabilized behavior than other pipes with nonzero values of power-law index.

The gravity effect is studied by generating results at different values of dimensionless gravity parameter κ. This parameter is a measure of weight of pipe and fluid and has negative, zero and positive values for upstanding, horizontal and down standing pipes, respectively. The results suggest that critical flow velocity is an increasing function of κ. To justify this fact, it should be mentioned that higher κ-value results in larger restoring force which correspondingly yields more stabilized system. Moreover, the presented Argand diagrams show that the variations in eigenfrequencies in different modes preserve the trend as α, κ or both change.

The D-R-D behavior represented by S-shaped regions in u_{cr}-β_f plots implies that the system restabilizes at velocities beyond u_{cr} and then destabilizes again with further increase in velocity. This behavior is also identifiable from Argand diagrams when a curve intersects $\mathrm{Re}(\omega)$ axis at three points. Inspecting the D-R-D regions, it can be concluded that these regions are formed as the composition of the pipe becomes or gets close to homogeneous. D-R-D regions are clearly be seen in all values of κ in the plots related to fully ceramic or fully metal pipes and also at $\alpha = 0.5$ and 1 at certain values of κ.

REFERENCES

Abdollahi, R., Dehghani Firouz-abadi, R., and Rahmanian, M., "On the stability of rotating pipes conveying fluid in annular liquid medium", *Journal of Sound and Vibration*, Vol. 494, pp. 115891 (2021).

Abo-bakr, H. M., Abo-bakr, R. M., Mohamed, S. A., and Eltaher, M. A., "Multi-objective shape optimization for axially functionally graded microbeams", *Composite Structures*, Vol. 258, pp. 113370 (2021).

Aghazadeh, R., "Torsional dynamics of bi-directional functionally graded small-scale tubes possessing a variable length scale parameter", *Mechanics of Advanced Materials and Structures*, pp. 1-8 (2020).

Aghazadeh, R., "Dynamics of axially functionally graded pipes conveying fluid using a higher order shear deformation theory", *International Advanced Researches and Engineering Journal*, Vol. 5, No. 2, pp. 209-217 (2021).

Aghazadeh, R., Dag, S., and Cigeroglu, E., "Modelling of graded rectangular micro-plates with variable length scale parameters", *Structural engineering and mechanics : An international journal*, Vol.

65, No. 5, pp. 573-585 (2018).

An, C., and Su, J., "Dynamic Behavior of Axially Functionally Graded Pipes Conveying Fluid", *Mathematical Problems in Engineering*, Vol. 2017, pp. 6789634 (2017).

Chen, W., Hu, Z., Dai, H., and Wang, L., "Extremely large-amplitude oscillation of soft pipes conveying fluid under gravity", *Applied Mathematics and Mechanics*, Vol. 41, No. 9, pp. 1381-1400 (2020).

Dagli, B. Y., and Ergut, A., "Dynamics of fluid conveying pipes using Rayleigh theory under non-classical boundary conditions", *European Journal of Mechanics - B/Fluids*, Vol. 77, pp. 125-134 (2019).

Dai, J., Liu, Y., Liu, H., Miao, C., and Tong, G., "A parametric study on thermo-mechanical vibration of axially functionally graded material pipe conveying fluid", *International Journal of Mechanics and Materials in Design*, Vol. 15, No. 4, pp. 715-726 (2019).

Dehrouyeh-Semnani, A. M., Dehdashti, E., Yazdi, M. R. H., and Nikkhah-Bahrami, M., "Nonlinear thermo-resonant behavior of fluid-conveying FG pipes", *International Journal of Engineering Science*, Vol. 144, pp. 103141 (2019).

Deng, J., Liu, Y., Zhang, Z., and Liu, W., "Stability analysis of multi-span viscoelastic functionally graded material pipes conveying fluid using a hybrid method", *European Journal of Mechanics - A/Solids*, Vol. 65, pp. 257-270 (2017).

Ebrahimi-Mamaghani, A., Sotudeh-Gharebagh, R., Zarghami, R., and Mostoufi, N., "Dynamics of two-phase flow in vertical pipes", *Journal of Fluids and Structures*, Vol. 87, pp. 150-173 (2019).

Ebrahimi-Mamaghani, A., Sotudeh-Gharebagh, R., Zarghami, R., and Mostoufi, N., "Thermo-mechanical stability of axially graded Rayleigh pipes", *Mechanics Based Design of Structures and Machines*, pp. 1-30 (2020).

ElNajjar, J., and Daneshmand, F., "Stability of horizontal and vertical pipes conveying fluid under the effects of additional point masses and springs", *Ocean Engineering*, Vol. 206, pp. 106943 (2020).

Ge, X., Li, Y., Chen, X., Shi, X., Ma, H., Yin, H., . . . Yang, C., "Dynamics of a Partially Confined, Vertical Upward-Fluid-Conveying, Slender Cantilever Pipe with Reverse External Flow", *Applied Sciences*, Vol. 9, No. 7, pp. 1425 (2019).

Ghayesh, M. H., "Nonlinear vibration analysis of axially functionally graded shear-deformable tapered beams", *Applied Mathematical Modelling*, Vol. 59, pp. 583-596 (2018).

Jiang, T., Dai, H., and Wang, L., "Three-dimensional dynamics of fluid-conveying pipe simultaneously subjected to external axial flow", *Ocean Engineering*, Vol. 217, pp. 107970 (2020).

Khodabakhsh, R., Saidi, A. R., and Bahaadini, R., "An analytical solution for nonlinear vibration and post-buckling of functionally graded pipes conveying fluid considering the rotary inertia and shear deformation effects", *Applied Ocean Research*, Vol. 101, pp. 102277 (2020).

Lee, U., and Park, J., "Spectral element modelling and analysis of a pipeline conveying internal unsteady fluid", *Journal of Fluids and Structures*, Vol. 22, No. 2, pp. 273-292 (2006).

Li, Q., Liu, W., Lu, K., and Yue, Z., "Flow-induced buckling statics and dynamics of imperfect pipes", *Archive of Applied Mechanics*, (2021).

Li, X., Li, L., Hu, Y., Ding, Z., and Deng, W., "Bending, buckling and vibration of axially functionally graded beams based on nonlocal strain gradient theory", *Composite Structures*, Vol. 165, pp. 250-265 (2017).

Li, Y.-d., and Yang, Y.-r., "Forced vibration of pipe conveying fluid by the Green function method", *Archive of Applied Mechanics*, Vol. 84, No. 12, pp. 1811-1823 (2014).

Liu, H., Lv, Z., and Tang, H., "Nonlinear vibration and instability of functionally graded nanopipes with initial imperfection conveying fluid", *Applied Mathematical Modelling*, Vol. 76, pp. 133-150 (2019).

Lu, Z.-Q., Zhang, K.-K., Ding, H., and Chen, L.-Q., "Nonlinear vibration effects on the fatigue life of fluid-conveying pipes composed of axially functionally graded materials", *Nonlinear Dynamics*, Vol. 100, No. 2, pp. 1091-1104 (2020).

Mahamood, R. M., and Akinlabi, E. T. (2017). Types of Functionally Graded Materials and Their Areas of Application. In R. M. Mahamood & E. T. Akinlabi (Eds.), *Functionally Graded Materials* (pp. 9-21). Cham: Springer International Publishing.

Mirtalebi, S. H., Ebrahimi-Mamaghani, A., and Ahmadian, M. T., "Vibration Control and Manufacturing of Intelligibly Designed Axially Functionally Graded Cantilevered Macro/Micro-tubes", *IFAC-PapersOnLine*, Vol. 52, No. 10, pp. 382-387 (2019).

Paidoussis, M. P., Fluid-Structure Interactions: Slender Structures and Axial Flow, Academic Press, London (1998).

Peng, G., Xiong, Y., Gao, Y., Liu, L., Wang, M., and Zhang, Z., "Non-linear dynamics of a simply supported fluid-conveying pipe subjected to motion-limiting constraints: Two-dimensional analysis", *Journal of Sound and Vibration*, Vol. 435, pp. 192-204 (2018).

Petit, C., Montanaro, L., and Palmero, P., "Functionally graded ceramics for biomedical application: Concept, manufacturing, and properties", *International Journal of Applied Ceramic Technology*, Vol. 15, No. 4, pp. 820-840 (2018).

Reddy, R. S., Panda, S., and Natarajan, G., "Nonlinear dynamics of functionally graded pipes conveying hot fluid", *Nonlinear Dynamics*, Vol. 99, No. 3, pp. 1989-2010 (2020).

Rivero-Rodriguez, J., and Pérez-Saborid, M., "Numerical investigation of the influence of gravity on flutter of cantilevered pipes conveying fluid", *Journal of Fluids and Structures*, Vol. 55, pp. 106-121 (2015).

Sadeghi-Goughari, M., Jeon, S., and Kwon, H.-J., "Fluid structure interaction of cantilever micro and nanotubes conveying magnetic fluid with small size effects under a transverse magnetic field", *Journal of Fluids and Structures*, Vol. 94, pp. 102951 (2020).

Sadeghi, M. H., and Karimi-Dona, M. H., "Dynamic behavior of a fluid conveying pipe subjected to a moving sprung mass – An FEM-state space approach", *International Journal of Pressure Vessels and Piping*, Vol. 88, No. 4, pp. 123-131 (2011).

Schwengber, A., Prado, H. J., Zilli, D. A., Bonelli, P. R., and Cukierman, A. L., "Carbon nanotubes buckypapers for potential transdermal drug delivery", *Materials Science and Engineering: C*, Vol. 57, pp. 7-13 (2015).

Szmidt, T., Pisarski, D., and Konowrocki, R., "Semi-active stabilisation of a pipe conveying fluid using eddy-current dampers: state-feedback control design, experimental validation", *Meccanica*, Vol. 54, No. 6, pp. 761-777 (2019).

Tang, Y., Lv, X., and Yang, T., "Bi-directional functionally graded beams: asymmetric modes and nonlinear free vibration", *Composites Part B: Engineering*, Vol. 156, pp. 319-331 (2019).

Tang, Y., Ma, Z.-S., Ding, Q., and Wang, T., "Dynamic interaction between bi-directional functionally graded materials and magneto-electro-elastic fields: A nano-structure analysis", *Composite Structures*, Vol. 264, pp. 113746 (2021).

Tang, Y., Wang, T., Ma, Z.-S., and Yang, T., "Magneto-electro-elastic modelling and nonlinear vibration analysis of bi-directional functionally graded beams", *Nonlinear*

Dynamics, Vol. 105, No. 3, pp. 2195-2227 (2021).

Tang, Y., Wang, T., and Zheng, Y., "Thermal effect on wave propagation behavior of viscoelastic carbon nanotubes conveying fluid with the spinning and longitudinal motions", *Modern Physics Letters B*, Vol. 35, No. 02, pp. 2150052 (2020).

Tang, Y., and Yang, T., "Bi-Directional Functionally Graded Nanotubes: Fluid Conveying Dynamics", *International Journal of Applied Mechanics*, Vol. 10, No. 04, pp. 1850041 (2018a).

Tang, Y., and Yang, T., "Post-buckling behavior and nonlinear vibration analysis of a fluid-conveying pipe composed of functionally graded material", *Composite Structures*, Vol. 185, pp. 393-400 (2018b).

Tang, Y., Yang, T., and Fang, B., "Fractional Dynamics of Fluid-Conveying Pipes Made of Polymer-Like Materials", *Acta Mechanica Solida Sinica*, Vol. 31, No. 2, pp. 243-258 (2018).

Tang, Y., Zhen, Y., and Fang, B., "Nonlinear vibration analysis of a fractional dynamic model for the viscoelastic pipe conveying fluid", *Applied Mathematical Modelling*, Vol. 56, pp. 123-136 (2018).

Xu, M. R., Xu, S. P., and Guo, H. Y., "Determination of natural frequencies of fluid-conveying pipes using homotopy perturbation method", *Computers & Mathematics with Applications*, Vol. 60, No. 3, pp. 520-527 (2010).

Zhang, T., Ouyang, H., Zhang, Y. O., and Lv, B. L., "Nonlinear dynamics of straight fluid-conveying pipes with general boundary conditions and additional springs and masses", *Applied Mathematical Modelling*, Vol. 40, No. 17, pp. 7880-7900 (2016).

Zhao, Y., Hu, D., Wu, S., Long, X., and Liu, Y., "Dynamics of axially functionally graded conical pipes conveying fluid", *Journal of Mechanics*, Vol. 37, pp. 318-326 (2021).

Zhen, Y., Gong, Y., and Tang, Y., "Nonlinear vibration analysis of a supercritical fluid-conveying pipe made of functionally graded material with initial curvature", *Composite Structures*, Vol. 268, pp. 113980 (2021).

Zhou, X.-w., Dai, H.-L., and Wang, L., "Dynamics of axially functionally graded cantilevered pipes conveying fluid", *Composite Structures*, Vol. 190, pp. 112-118 (2018).

Zhu, B., Chen, X.-C., Guo, Y., and Li, Y.-H., "Static and dynamic characteristics of the post-buckling of fluid-conveying porous functionally graded pipes with geometric imperfections", *International Journal of Mechanical Sciences*, Vol. 189, pp. 105947 (2021).

Zhu, B., Xu, Q., Li, M., and Li, Y., "Nonlinear free and forced vibrations of porous functionally graded pipes conveying fluid and resting on nonlinear elastic foundation", *Composite Structures*, Vol. 252, pp. 112672 (2020).